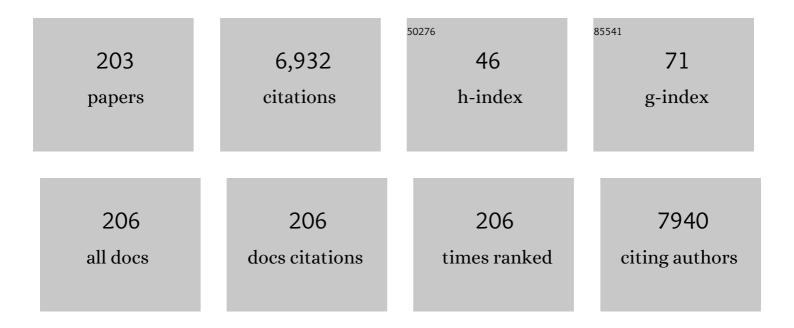
Th Strunskus

List of Publications by Year in descending order

Source: https://exaly.com/author-pdf/9063285/publications.pdf Version: 2024-02-01



#	Article	IF	CITATIONS
1	Free Volume and Transport Properties in Highly Selective Polymer Membranes. Macromolecules, 2002, 35, 2071-2077.	4.8	239
2	Metalâ€Polymer Nanocomposites for Functional Applications. Advanced Engineering Materials, 2010, 12, 1177-1190.	3.5	209
3	Covalent Interlinking of an Aldehyde and an Amine on a Au(111) Surface in Ultrahigh Vacuum. Angewandte Chemie - International Edition, 2007, 46, 9227-9230.	13.8	191
4	Deprotonation-Driven Phase Transformations in Terephthalic Acid Self-Assembly on Cu(100). Journal of Physical Chemistry B, 2004, 108, 19392-19397.	2.6	156
5	Enhanced ethanol vapour sensing performances of copper oxide nanocrystals with mixed phases. Sensors and Actuators B: Chemical, 2016, 224, 434-448.	7.8	140
6	Layer-by-Layer Growth of Oriented Metal Organic Polymers on a Functionalized Organic Surface. Langmuir, 2007, 23, 7440-7442.	3.5	127
7	Conformational Adaptation and Selective Adatom Capturing of Tetrapyridyl-porphyrin Molecules on a Copper (111) Surface. Journal of the American Chemical Society, 2007, 129, 11279-11285.	13.7	122
8	Ionic Hydrogen Bonds Controlling Two-Dimensional Supramolecular Systems at a Metal Surface. Chemistry - A European Journal, 2007, 13, 3900-3906.	3.3	117
9	Real-Time Monitoring of Morphology and Optical Properties during Sputter Deposition for Tailoring Metal–Polymer Interfaces. ACS Applied Materials & Interfaces, 2015, 7, 13547-13556.	8.0	113
10	Tunable multiple plasmon resonance wavelengths response from multicomponent polymer-metal nanocomposite systems. Applied Physics Letters, 2004, 84, 2655-2657.	3.3	112
11	Free Volume Distributions in Glassy Polymer Membranes:Â Comparison between Molecular Modeling and Experiments. Macromolecules, 2000, 33, 2242-2248.	4.8	102
12	Metal/polymer interfaces with designed morphologies. Journal of Adhesion Science and Technology, 2000, 14, 467-490.	2.6	97
13	Visualizing the Frontier Orbitals of a Conformationally Adapted Metalloporphyrin. ChemPhysChem, 2008, 9, 89-94.	2.1	96
14	Plasmonic tunable metamaterial absorber as ultraviolet protection film. Applied Physics Letters, 2014, 104, .	3.3	95
15	Importance of dewetting in organic molecular-beam deposition: Pentacene on gold. Applied Physics Letters, 2004, 85, 398-400.	3.3	94
16	Combined STM and FTIR Characterization of Terphenylalkanethiol Monolayers on Au(111):  Effect of Alkyl Chain Length and Deposition Temperature. Langmuir, 2006, 22, 3647-3655.	3.5	94
17	Identification of Physical and Chemical Interaction Mechanisms for the Metals Gold, Silver, Copper, Palladium, Chromium, and Potassium with Polyimide Surfaces. Langmuir, 1996, 12, 2712-2725.	3.5	92
18	Competition as a Design Concept:Â Polymorphism in Self-Assembled Monolayers of Biphenyl-Based Thiols. Journal of the American Chemical Society, 2006, 128, 13868-13878.	13.7	91

#	Article	IF	CITATIONS
19	Embedding of Noble Metal Nanoclusters into Polymers as a Potential Probe of the Surface Glass Transition. Macromolecules, 2001, 34, 1125-1127.	4.8	87
20	Polymer–metal optical nanocomposites with tunable particle plasmon resonance prepared by vapor phase co-deposition. Materials Letters, 2004, 58, 1530-1534.	2.6	78
21	Electronic structure of CuWO4: XPS, XES and NEXAFS studies. Journal of Alloys and Compounds, 2005, 389, 14-20.	5.5	76
22	Photodeposition of Au Nanoclusters for Enhanced Photocatalytic Dye Degradation over TiO ₂ Thin Film. ACS Applied Materials & Interfaces, 2020, 12, 14983-14992.	8.0	75
23	Linear dichroism in X-ray absorption spectroscopy of strongly chemisorbed planar molecules: role of adsorption induced rehybridisations. Surface Science, 1995, 341, L1055-L1060.	1.9	74
24	Controlled Generation of Ni Nanoparticles in the Capping Layers of Teflon AF by Vapor-Phase Tandem Evaporation. Nano Letters, 2003, 3, 69-73.	9.1	72
25	Towards large-scale in free-standing graphene and N-graphene sheets. Scientific Reports, 2017, 7, 10175.	3.3	71
26	Coexistence of one- and two-dimensional supramolecular assemblies of terephthalic acid on Pd(111) due to self-limiting deprotonation. Journal of Chemical Physics, 2006, 125, 184710.	3.0	66
27	Condensation coefficients and initial stages of growth for noble metals deposited onto chemically different polymer surfaces. Applied Surface Science, 1999, 144-145, 355-359.	6.1	65
28	N-Graphene Nanowalls via Plasma Nitrogen Incorporation and Substitution: The Experimental Evidence. Nano-Micro Letters, 2020, 12, 53.	27.0	65
29	Role of Sputter Deposition Rate in Tailoring Nanogranular Gold Structures on Polymer Surfaces. ACS Applied Materials & Interfaces, 2017, 9, 5629-5637.	8.0	64
30	Resolving the depth coordinate in photoelectron spectroscopy – Comparison of excitation energy variation vs. angular-resolved XPS for the analysis of a self-assembled monolayer model system. Surface Science, 2008, 602, 755-767.	1.9	61
31	Fabrication of Self-Assembled Monolayers Exhibiting a Thiol-Terminated Surface. Langmuir, 2004, 20, 8620-8624.	3.5	60
32	Influence of Molecular Structure on Phase Transitions:  A Study of Self-Assembled Monolayers of 2-(Aryl)-ethane Thiols. Journal of Physical Chemistry C, 2007, 111, 16909-16919.	3.1	60
33	Formation of metal–polymer interfaces by metal evaporation: influence of deposition parameters and defects. Microelectronic Engineering, 2000, 50, 465-471.	2.4	59
34	A comparative study of photocatalysis on highly active columnar TiO2 nanostructures in-air and in-solution. Solar Energy Materials and Solar Cells, 2018, 178, 170-178.	6.2	59
35	Pathways to Tailor Photocatalytic Performance of TiO2 Thin Films Deposited by Reactive Magnetron Sputtering. Materials, 2019, 12, 2840.	2.9	59
36	Rational Design of Two-Dimensional Nanoscale Networks by Electrostatic Interactions at Surfaces. ACS Nano, 2010, 4, 1813-1820.	14.6	58

#	Article	IF	CITATIONS
37	Tuning of electrical and structural properties of metal-polymer nanocomposite films prepared by co-evaporation technique. Applied Physics A: Materials Science and Processing, 2008, 92, 345-350.	2.3	57
38	Photocatalytic properties of titania thin films prepared by sputtering versus evaporation and aging of induced oxygen vacancy defects. Applied Catalysis B: Environmental, 2016, 180, 362-371.	20.2	54
39	Azobenzene-Containing Triazatriangulenium Adlayers on Au(111): Structural and Spectroscopic Characterization. Langmuir, 2011, 27, 5899-5908.	3.5	53
40	Single target sputter deposition of alloy nanoparticles with adjustable composition via a gas aggregation cluster source. Nanotechnology, 2017, 28, 175703.	2.6	52
41	Monitoring the reversible photoisomerization of an azobenzene-functionalized molecular triazatriangulene platform on Au(111) by IRRAS. Physical Chemistry Chemical Physics, 2014, 16, 22643-22650.	2.8	50
42	Size dependent characteristics of plasma synthesized carbonaceous nanoparticles. Journal of Applied Physics, 2012, 112, .	2.5	49
43	Functional Polymer Nanocomposites. Polymers and Polymer Composites, 2008, 16, 471-481.	1.9	48
44	Effect of gold alloying on stability of silver nanoparticles and control of silver ion release from vapor-deposited Ag–Au/polytetrafluoroethylene nanocomposites. Gold Bulletin, 2013, 46, 3-11.	2.4	48
45	Giant magnetoelectric effect at low frequencies in polymer-based thin film composites. Applied Physics Letters, 2014, 104, .	3.3	48
46	Preparation and plasmonic properties of polymer-based composites containing Ag–Au alloy nanoparticles produced by vapor phase co-deposition. Journal of Materials Science, 2010, 45, 5865-5871.	3.7	47
47	From Au–Thiolate Chains to Thioether Sierpiński Triangles: The Versatile Surface Chemistry of 1,3,5-Tris(4-mercaptophenyl)benzene on Au(111). ACS Nano, 2016, 10, 10901-10911.	14.6	47
48	(CuO-Cu2O)/ZnO:Al heterojunctions for volatile organic compound detection. Sensors and Actuators B: Chemical, 2018, 255, 1362-1375.	7.8	47
49	Asymmetry Induction by Cooperative Intermolecular Hydrogen Bonds in Surface-Anchored Layers of Achiral Molecules. ChemPhysChem, 2006, 7, 2197-2204.	2.1	46
50	Tuning of the ion release properties of silver nanoparticles buried under a hydrophobic polymer barrier. Journal of Nanoparticle Research, 2012, 14, 1.	1.9	46
51	Magnetron-sputtered copper nanoparticles: lost in gas aggregation and found by <i>in situ</i> X-ray scattering. Nanoscale, 2018, 10, 18275-18281.	5.6	46
52	Investigation of the Surface Glass Transition Temperature by Embedding of Noble Metal Nanoclusters into Monodisperse Polystyrenes. Macromolecules, 2004, 37, 1831-1838.	4.8	45
53	Surface topography and wetting modifications of PEEK for implant applications. Lasers in Medical Science, 2014, 29, 1633-1639.	2.1	45
54	Influence of reactive gas admixture on transition metal cluster nucleation in a gas aggregation cluster source. Journal of Applied Physics, 2012, 112, .	2.5	44

#	Article	IF	CITATIONS
55	Chemistry, diffusion and cluster formation at metal-polymer interfaces. Materials and Corrosion - Werkstoffe Und Korrosion, 1998, 49, 180-188.	1.5	43
56	Evidence of noble metal diffusion in polymers at room temperature and its retardation by a chromium barrier. Applied Physics Letters, 2002, 81, 244-246.	3.3	43
57	XES, XPS and NEXAFS studies of the electronic structure of cubic MoO1.9 and H1.63MoO3 thick films. Journal of Alloys and Compounds, 2004, 366, 54-60.	5.5	43
58	Conformational Adaptation in Supramolecular Assembly on Surfaces. ChemPhysChem, 2007, 8, 1782-1786.	2.1	41
59	Anomalous Surface Compositions of Stoichiometric Mixed Oxide Compounds. Angewandte Chemie - International Edition, 2010, 49, 8037-8041.	13.8	41
60	Reactivity of ZnO Surfaces toward Maleic Anhydride. Journal of Physical Chemistry B, 2004, 108, 13736-13745.	2.6	40
61	Organic molecular-beam deposition of perylene on Cu(110): Results from near-edge x-ray absorption spectroscopy, x-ray photoelectron spectroscopy, and atomic force microscopy. Journal of Materials Research, 2004, 19, 2049-2056.	2.6	40
62	Valence band electronic structure of V2O5 as determined by resonant soft X-ray emission spectroscopy. Journal of Electron Spectroscopy and Related Phenomena, 2005, 149, 45-50.	1.7	40
63	Mass Spectrometric Investigations of Nanoâ€Size Cluster Ions Produced by High Pressure Magnetron Sputtering. Contributions To Plasma Physics, 2012, 52, 881-889.	1.1	40
64	Microstructural and plasmonic modifications in Ag–TiO ₂ and Au–TiO ₂ nanocomposites through ion beam irradiation. Beilstein Journal of Nanotechnology, 2014, 5, 1419-1431.	2.8	40
65	Postâ€Synthetic Decoupling of Onâ€Surfaceâ€Synthesized Covalent Nanostructures from Ag(111). Angewandte Chemie - International Edition, 2016, 55, 7650-7654.	13.8	39
66	Light-Controlled Conductance Switching in Azobenzene-Containing MWCNT–Polymer Nanocomposites. ACS Applied Materials & Interfaces, 2015, 7, 11257-11262.	8.0	38
67	Correlating Nanostructure, Optical and Electronic Properties of Nanogranular Silver Layers during Polymer-Template-Assisted Sputter Deposition. ACS Applied Materials & Interfaces, 2019, 11, 29416-29426.	8.0	37
68	Whey protein hydrolysates reduce autoxidation in microencapsulated long chain polyunsaturated fatty acids. European Journal of Lipid Science and Technology, 2015, 117, 1960-1970.	1.5	36
69	Tuning doping and surface functionalization of columnar oxide films for volatile organic compound sensing: experiments and theory. Journal of Materials Chemistry A, 2018, 6, 23669-23682.	10.3	36
70	Huge increase in gas phase nanoparticle generation by pulsed direct current sputtering in a reactive gas admixture. Applied Physics Letters, 2013, 103, .	3.3	35
71	Role of UV Plasmonics in the Photocatalytic Performance of TiO ₂ Decorated with Aluminum Nanoparticles. ACS Applied Nano Materials, 2018, 1, 3760-3764.	5.0	35
72	Antibacterial, highly hydrophobic and semi transparent Ag/plasma polymer nanocomposite coating on cotton fabric obtained by plasma based co-deposition. Cellulose, 2019, 26, 8877-8894.	4.9	34

#	Article	IF	CITATIONS
73	Does the Surface Matter? Hydrogenâ€Bonded Chain Formation of an Oxalic Amide Derivative in a Two― and Threeâ€Dimensional Environment. ChemPhysChem, 2008, 9, 2522-2530.	2.1	32
74	Uniform Ï€â€System Alignment in Thin Films of Templateâ€Grown Dicarbonitrileâ€Oligophenyls. Advanced Functional Materials, 2011, 21, 1631-1642.	14.9	32
75	Plasma-polymerized HMDSO coatings to adjust the silver ion release properties of Ag/polymer nanocomposites. Journal of Nanoparticle Research, 2013, 15, 1.	1.9	32
76	Self-Assembled Monolayers of Benzylmercaptan and <i>p</i> -Cyanobenzylmercaptan on Au(111) Surfaces: Structural and Spectroscopic Characterization. Langmuir, 2008, 24, 5726-5733.	3.5	31
77	Evidence of Aggregation-Induced Copper Immobilization During Polyimide Metallization. Advanced Materials, 1998, 10, 1357-1360.	21.0	30
78	Nucleation and Growth of Magnetron‣puttered Ag Nanoparticles as Witnessed by Timeâ€Resolved Small Angle Xâ€Ray Scattering. Particle and Particle Systems Characterization, 2020, 37, 1900436.	2.3	30
79	Supramolecular Organization and Chiral Resolution of <i>p</i> â€Terphenylâ€ <i>m</i> â€Dicarbonitrile on the Ag(111) Surface. ChemPhysChem, 2010, 11, 1446-1451.	2.1	29
80	On-Surface Polymerization of 1,6-Dibromo-3,8-diiodpyrene—A Comparative Study on Au(111) Versus Ag(111) by STM, XPS, and NEXAFS. Journal of Physical Chemistry C, 2018, 122, 5967-5977.	3.1	29
81	Plasma based formation and deposition of metal and metal oxide nanoparticles using a gas aggregation source. European Physical Journal D, 2018, 72, 1.	1.3	29
82	Condensation coefficients of noble metals on polymers: a novel method of determination by x-ray photoelectron spectroscopy. Surface and Interface Analysis, 2000, 30, 439-443.	1.8	28
83	Molecular dynamics simulation of gold cluster growth during sputter deposition. Journal of Applied Physics, 2016, 119, .	2.5	28
84	Tunable polytetrafluoroethylene electret films with extraordinary charge stability synthesized by initiated chemical vapor deposition for organic electronics applications. Scientific Reports, 2019, 9, 2237.	3.3	28
85	Low-temperature low-power PECVD synthesis of vertically aligned graphene. Nanotechnology, 2020, 31, 395604.	2.6	28
86	Reversible light-controlled conductance switching of azobenzene-based metal/polymer nanocomposites. Nanotechnology, 2010, 21, 465201.	2.6	27
87	Surface segregation in TiO ₂ -based nanocomposite thin films. Nanotechnology, 2012, 23, 495701.	2.6	27
88	Tailoring the Morphology of Metal/Polymer Interfaces. Advanced Engineering Materials, 2000, 2, 489-492.	3.5	26
89	X-ray spectroscopy characterization of azobenzene-functionalized triazatriangulenium adlayers on Au(111) surfaces. Physical Chemistry Chemical Physics, 2015, 17, 17053-17062.	2.8	26
90	Plasmonic and non-plasmonic contributions on photocatalytic activity of Au-TiO2 thin film under mixed UV–visible light. Surface and Coatings Technology, 2020, 389, 125613.	4.8	26

#	Article	IF	CITATIONS
91	Self-assembled monolayers of benzylmercaptan and para-cyanobenzylmercaptan on gold: surface infrared spectroscopic characterization. Physical Chemistry Chemical Physics, 2010, 12, 4390.	2.8	25
92	Metal/polymer nanocomposite thin films prepared by plasma polymerization and high pressure magnetron sputtering. Surface and Coatings Technology, 2011, 205, S38-S41.	4.8	25
93	Longâ€Distance Rate Acceleration by Bulk Gold. Angewandte Chemie - International Edition, 2019, 58, 6574-6578.	13.8	25
94	Cauliflower-like CeO ₂ –TiO ₂ hybrid nanostructures with extreme photocatalytic and self-cleaning properties. Nanoscale, 2019, 11, 9840-9844.	5.6	24
95	Real-time insight into nanostructure evolution during the rapid formation of ultra-thin gold layers on polymers. Nanoscale Horizons, 2021, 6, 132-138.	8.0	24
96	Metallization of a Thiol-Terminated Organic Surface Using Chemical Vapor Deposition. Langmuir, 2008, 24, 7986-7994.	3.5	23
97	Plasmonic properties of vapour-deposited polymer composites containing Ag nanoparticles and their changes upon annealing. Journal Physics D: Applied Physics, 2008, 41, 125409.	2.8	23
98	Study of cobalt clusters with very narrow size distribution deposited by high-rate cluster source. Nanotechnology, 2011, 22, 465704.	2.6	23
99	Diffusive Memristive Switching on the Nanoscale, from Individual Nanoparticles towards Scalable Nanocomposite Devices. Scientific Reports, 2019, 9, 17367.	3.3	23
100	Light-induced conductance switching in azobenzene based near-percolated single wall carbon nanotube/polymer composites. Carbon, 2015, 90, 94-101.	10.3	22
101	Durability of resin bonding to zirconia ceramic after contamination and the use of various cleaning methods. Dental Materials, 2019, 35, 1388-1396.	3.5	22
102	PdO nanoparticles decorated TiO2 film with enhanced photocatalytic and self-cleaning properties. Materials Today Chemistry, 2020, 16, 100251.	3.5	22
103	Kinetically Stable, Flat-Lying Thiolate Monolayers. Angewandte Chemie - International Edition, 2007, 46, 3762-3764.	13.8	21
104	Formation and material analysis of plasma polymerized carbon nitride nanoparticles. Journal of Applied Physics, 2009, 105, .	2.5	21
105	Vapor Phase Deposition, Structure, and Plasmonic Properties of Polymer-Based Composites Containing Ag–Cu Bimetallic Nanoparticles. Plasmonics, 2012, 7, 107-114.	3.4	21
106	High rate deposition system for metal-cluster/SiO x C y H z –polymer nanocomposite thin films. Journal of Nanoparticle Research, 2013, 15, 1.	1.9	21
107	Role of oxygen admixture in stabilizing TiO x nanoparticle deposition from a gas aggregation source. Journal of Nanoparticle Research, 2013, 15, 1.	1.9	21
108	Electret films with extremely high charge stability prepared by thermal evaporation of Teflon AF. Organic Electronics, 2018, 57, 146-150.	2.6	21

#	Article	IF	CITATIONS
109	Photocatalytic Growth of Hierarchical Au Needle Clusters on Highly Active TiO ₂ Thin Film. Advanced Materials Interfaces, 2018, 5, 1800465.	3.7	21
110	The method of conventional calorimetric probes — A short review and application for the characterization of nanocluster sources. Surface and Coatings Technology, 2011, 205, S388-S392.	4.8	20
111	Ultra-fast degradation of methylene blue by Au/ZnO-CeO2 nano-hybrid catalyst. Materials Letters, 2017, 209, 486-491.	2.6	20
112	Self-organized nanocrack networks: a pathway to enlarge catalytic surface area in sputtered ceramic thin films, showcased for photocatalytic TiO ₂ . Nanotechnology, 2018, 29, 035703.	2.6	20
113	The impact of O ₂ /Ar ratio on morphology and functional properties in reactive sputtering of metal oxide thin films. Nanotechnology, 2019, 30, 235603.	2.6	20
114	Nanoscale gradient copolymer films via single-step deposition from the vapor phase. Materials Today, 2020, 37, 35-42.	14.2	20
115	A Flexible Oxygenated Carbographite Nanofilamentous Buckypaper as an Amphiphilic Membrane. Advanced Materials Interfaces, 2018, 5, 1800001.	3.7	19
116	Remote functionalization in surface-assisted dehalogenation by conformational mechanics: organometallic self-assembly of 3,3′,5,5′-tetrabromo-2,2′,4,4′,6,6′-hexafluorobiphenyl on Ag(111). Nanoscale, 2018, 10, 12035-12044.	5.6	19
117	Superhydrophobic 3D Porous PTFE/TiO ₂ Hybrid Structures. Advanced Materials Interfaces, 2019, 6, 1801967.	3.7	19
118	Concept and modelling of memsensors as two terminal devices with enhanced capabilities in neuromorphic engineering. Scientific Reports, 2019, 9, 4361.	3.3	19
119	Epileptic Seizure Detection on an Ultra-Low-Power Embedded RISC-V Processor Using a Convolutional Neural Network. Biosensors, 2021, 11, 203.	4.7	19
120	Organic Molecular Beam Deposition of Oligophenyls on Au(111): A Study by X-ray Absorption Spectroscopy. ChemPhysChem, 2006, 7, 2552-2558.	2.1	18
121	Chemistry in Confined Geometries: Reactions at an Organic Surface. ChemPhysChem, 2007, 8, 657-660.	2.1	18
122	Optical switching behavior of azobenzene/PMMA blends with high chromophore concentration. Journal of Materials Science, 2011, 46, 2488-2494.	3.7	18
123	Efficacy of Plasma Treatment for Decontaminating Zirconia. Journal of Adhesive Dentistry, 2018, 20, 289-297.	0.5	17
124	Metalâ^'Organic Chemical Vapor Deposition of Palladium:  Spectroscopic Study of Cyclopentadienyl-allyl-palladium Deposition on a Palladium Substrate. Chemistry of Materials, 2005, 17, 861-868.	6.7	16
125	Formation of magnetic nanocolumns during vapor phase deposition of a metal-polymer nanocomposite: Experiments and kinetic Monte Carlo simulations. Journal of Applied Physics, 2013, 114,	2.5	16
126	<i>In situ</i> Raman spectroscopy for growth monitoring of vertically aligned multiwall carbon nanotubes in plasma reactor. Applied Physics Letters, 2014, 105, .	3.3	16

#	Article	IF	CITATIONS
127	Tuning wettability of TiO2 thin film by photocatalytic deposition of 3D flower- and hedgehog-like Au nano- and microstructures. Applied Surface Science, 2021, 537, 147795.	6.1	16
128	The valence electronic structure of zinc oxide powders as determined by X-ray emission spectroscopy: variation of electronic structure with particle size. Journal of Electron Spectroscopy and Related Phenomena, 2004, 134, 183-189.	1.7	15
129	Electronic structure, adsorption geometry, and photoswitchability of azobenzene layers adsorbed on layered crystals. Physical Chemistry Chemical Physics, 2013, 15, 20272.	2.8	15
130	Ag Nanoparticles Decorated TiO 2 Thin Films with Enhanced Photocatalytic Activity. Physica Status Solidi (A) Applications and Materials Science, 2019, 216, 1800898.	1.8	15
131	Molecular adsorption and growth of naphthalene films on Ag(100). Surface Science, 2007, 601, 2089-2094.	1.9	14
132	Nanostructural and Functional Properties of Ag-TiO ₂ Coatings Prepared by Co-Sputtering Deposition Technique. Journal of Nanoscience and Nanotechnology, 2011, 11, 4893-4899.	0.9	14
133	Huge increase of therapeutic window at a bioactive silver/titania nanocomposite coating surface compared to solution. Materials Science and Engineering C, 2013, 33, 2367-2375.	7.3	14
134	Grafting of Functionalized [Fe(III)(salten)] Complexes to Au(111) Surfaces via Thiolate Groups: Surface Spectroscopic Characterization and Comparison of Different Linker Designs. Langmuir, 2013, 29, 8534-8543.	3.5	14
135	Controlling surface segregation of reactively sputtered Ag/TiOx nanocomposites. Acta Materialia, 2014, 74, 1-8.	7.9	14
136	Nanogenerator and piezotronic inspired concepts for energy efficient magnetic field sensors. Nano Energy, 2019, 56, 420-425.	16.0	14
137	Prospects for microwave plasma synthesized N-graphene in secondary electron emission mitigation applications. Scientific Reports, 2020, 10, 13013.	3.3	14
138	Selective Silver Nanocluster Metallization on Conjugated Diblock Copolymer Templates for Sensing and Photovoltaic Applications. ACS Applied Nano Materials, 2021, 4, 4245-4255.	5.0	14
139	CO2 Adlayers on the Mixed Terminated ZnO(10-10) Surface Studied by He Atom Scattering, Photoelectron Spectroscopy and Ab Initio Electronic Structure Calculations. Zeitschrift Fur Physikalische Chemie, 2008, 222, 891-915.	2.8	13
140	N-Graphene-Metal-Oxide(Sulfide) hybrid Nanostructures: Single-step plasma-enabled approach for energy storage applications. Chemical Engineering Journal, 2022, 430, 133153.	12.7	13
141	Controlled synthesis of germanium nanoparticles by nonthermal plasmas. Applied Physics Letters, 2016, 108, .	3.3	12
142	Fabrication of Diazocine-Based Photochromic Organic Thin Films via Initiated Chemical Vapor Deposition. Macromolecules, 2020, 53, 1164-1170.	4.8	12
143	Enhancing composition control of alloy nanoparticles from gas aggregation source by in operando optical emission spectroscopy. Plasma Processes and Polymers, 2021, 18, 2000208.	3.0	12
144	Highly versatile concept for precise tailoring of nanogranular composites with a gas aggregation cluster source. Applied Physics Letters, 2012, 100, .	3.3	11

#	Article	IF	CITATIONS
145	Biomimetic Transferable Surface for a Real Time Control over Wettability and Photoerasable Writing with Water Drop Lens. Scientific Reports, 2015, 4, 7407.	3.3	11
146	Light-induced Conductance Switching in Photomechanically Active Carbon Nanotube-Polymer Composites. Scientific Reports, 2017, 7, 9648.	3.3	11
147	Influence of a Metal Substrate on Smallâ€Molecule Activation Mediated by a Surfaceâ€Adsorbed Complex. Chemistry - A European Journal, 2018, 24, 10732-10744.	3.3	11
148	Revealing the growth of copper on polystyrene-block-poly(ethylene oxide) diblock copolymer thin films with in situ GISAXS. Nanoscale, 2021, 13, 10555-10565.	5.6	11
149	Brain-like critical dynamics and long-range temporal correlations in percolating networks of silver nanoparticles and functionality preservation after integration of insulating matrix. Nanoscale Advances, 2022, 4, 3149-3160.	4.6	11
150	Template-Induced Growth of Sputter-Deposited Gold Nanoparticles on Ordered Porous TiO ₂ Thin Films for Surface-Enhanced Raman Scattering Sensors. ACS Applied Nano Materials, 2022, 5, 7492-7501.	5.0	11
151	Reversible light-induced capacitance switching of azobenzene ether/PMMA blends. Applied Physics A: Materials Science and Processing, 2011, 102, 421-427.	2.3	10
152	Ordered Adlayers of a Combined Lateral Switch and Rotor. Journal of Physical Chemistry C, 2019, 123, 13720-13730.	3.1	10
153	Following in Situ the Deposition of Gold Electrodes on Low Band Gap Polymer Films. ACS Applied Materials & Interfaces, 2020, 12, 1132-1141.	8.0	10
154	Effect of composition and structure of gold/copper bimetallic nanoparticles on dispersion in polymer thin films. Journal of Materials Chemistry, 2002, 12, 3610-3614.	6.7	9
155	A critical evaluation of the 0–3 approach for magnetoelectric nanocomposites with metallic nanoparticles. Journal of Applied Physics, 2012, 112, 044303.	2.5	9
156	Enhancement of catalytic effect for CNT growth at low temperature by PECVD. Applied Surface Science, 2018, 453, 436-441.	6.1	9
157	Improving the Switching Capacity of Glycoâ€Selfâ€Assembled Monolayers on Au(111). Chemistry - A European Journal, 2020, 26, 485-501.	3.3	9
158	Synthesis and Investigation of a Photoswitchable Copolymer Deposited via Initiated Chemical Vapor Deposition for Application in Organic Smart Surfaces. ACS Applied Polymer Materials, 2021, 3, 1445-1456.	4.4	9
159	Molecular Insight into Real-Time Reaction Kinetics of Free Radical Polymerization from the Vapor Phase by In-Situ Mass Spectrometry. Journal of Physical Chemistry A, 2021, 125, 1661-1667.	2.5	9
160	Correlating Optical Reflectance with the Topology of Aluminum Nanocluster Layers Growing on Partially Conjugated Diblock Copolymer Templates. ACS Applied Materials & Interfaces, 2021, 13, 56663-56673.	8.0	9
161	Nucleation, growth, interdiffusion, and adhesion of metal films on polymers. AIP Conference Proceedings, 1999, , .	0.4	8
162	Free volume changes on optical switching in azobenzeneâ€polymethylmethacrylate blends studied by a pulsed lowâ€energy positron beam. Journal of Polymer Science, Part B: Polymer Physics, 2011, 49, 404-408.	2.1	8

#	Article	IF	CITATIONS
163	Formation of polymer-based nanoparticles and nanocomposites by plasma-assisted deposition methods. European Physical Journal D, 2018, 72, 1.	1.3	8
164	Longâ€Distance Rate Acceleration by Bulk Gold. Angewandte Chemie, 2019, 131, 6646-6650.	2.0	8
165	Sensing performance of CuO/Cu2O/ZnO:Fe heterostructure coated with thermally stable ultrathin hydrophobic PV3D3 polymer layer for battery application. Materials Today Chemistry, 2022, 23, 100642.	3.5	8
166	Mechanism of X-ray-induced degradation of pyromellitic dianhydride. Journal of Electron Spectroscopy and Related Phenomena, 1993, 61, 193-216.	1.7	7
167	In situ atomic force microscopy studies of reversible light-induced switching of surface roughness and adhesion in azobenzene-containing PMMA films. Applied Surface Science, 2011, 257, 7719-7726.	6.1	7
168	Simulation of nanocolumn formation in a plasma environment. Journal of Applied Physics, 2015, 117, 014305.	2.5	7
169	Quantitative Evaluation of Contamination on Dental Zirconia Ceramic by Silicone Disclosing Agents after Different Cleaning Procedures. Materials, 2015, 8, 2650-2657.	2.9	7
170	Tuning silver ion release properties in reactively sputtered Ag/TiOx nanocomposites. Applied Physics A: Materials Science and Processing, 2017, 123, 1.	2.3	7
171	Enhancing Reliability of Studies on Single Filament Memristive Switching via an Unconventional cAFM Approach. Nanomaterials, 2021, 11, 265.	4.1	7
172	Neutron spectroscopy study of the diffusivity of hydrogen in MoS ₂ . Physical Chemistry Chemical Physics, 2021, 23, 7961-7973.	2.8	7
173	Influence of Cleaning Methods on Resin Bonding to Contaminated Translucent 3Y-TZP ceramic. Journal of Adhesive Dentistry, 2020, 22, 383-391.	0.5	7
174	In Situ Monitoring of Scale Effects on Phase Selection and Plasmonic Shifts during the Growth of AgCu Alloy Nanostructures for Anticounterfeiting Applications. ACS Applied Nano Materials, 2022, 5, 3832-3842.	5.0	7
175	Nitrogen incorporation in graphene nanowalls via plasma processes: Experiments and simulations. Applied Surface Science, 2022, 591, 153165.	6.1	7
176	Morphological and magnetic properties of TiO2/Fe50Co50 composite films. Journal of Materials Science, 2011, 46, 4638-4645.	3.7	6
177	Combined in situ electrochemical impedance spectroscopy–UV/Vis and AFM studies of Ag nanoparticle stability in perfluorinated films. Materials Chemistry and Physics, 2012, 134, 302-308.	4.0	6
178	Evaporated electret films with superior charge stability based on Teflon AF 2400. Organic Electronics, 2019, 70, 167-171.	2.6	6
179	Impact of argon flow and pressure on the trapping behavior of nanoparticles inside a gas aggregation source. Plasma Processes and Polymers, 2022, 19, e2100125.	3.0	6
180	A thin-film broadband perfect absorber based on plasmonic copper nanoparticles. Micro and Nano Engineering, 2022, 16, 100154.	2.9	6

#	Article	IF	CITATIONS
181	Nanocomposites of Vapour Phase Deposited Teflon AF Containing Ni Clusters. Solid State Phenomena, 2003, 94, 285-294.	0.3	5
182	Simple method of hybrid PVD/PECVD to prepare well-dispersed cobalt–plasma polymerized hexamethyldisilazane nanocomposites. Surface and Coatings Technology, 2012, 207, 565-570.	4.8	5
183	Formation and behavior of negative ions in low pressure aniline-containing RF plasmas. Scientific Reports, 2019, 9, 10886.	3.3	5
184	Molybdenum tricarbonyl complex functionalised with a molecular triazatriangulene platform on Au(111): surface spectroscopic characterisation. Dalton Transactions, 2021, 50, 1042-1052.	3.3	5
185	Additive Manufacturing as a Means of Gas Sensor Development for Battery Health Monitoring. Chemosensors, 2021, 9, 252.	3.6	5
186	From Benzenetrithiolate Self-Assembly to Copper Sulfide Adlayers on Cu(111): Temperature-Induced Irreversible and Reversible Phase Transitions. Journal of Physical Chemistry C, 2014, 118, 3590-3598.	3.1	4
187	Tailoring the Optical Properties of Sputter-Deposited Gold Nanostructures on Nanostructured Titanium Dioxide Templates Based on In Situ Grazing-Incidence Small-Angle X-ray Scattering Determined Growth Laws. ACS Applied Materials & Interfaces, 2021, 13, 14728-14740.	8.0	4
188	Thermal stability studies of plasma deposited hydrogenated carbon nitride nanostructures. Carbon, 2021, 184, 82-90.	10.3	4
189	Kinetic Monte Carlo Simulations of Cluster Growth and Diffusion in Metal-Polymer Nanocomposites. Springer Series on Atomic, Optical, and Plasma Physics, 2014, , 321-370.	0.2	4
190	Monitoring magnetostriction by a quantum tunnelling strain sensor. Sensors and Actuators A: Physical, 2012, 183, 28-33.	4.1	3
191	Controlled deposition of plasmaâ€polyaniline thin film by PECVD: Understanding the influence of aniline to argon ratio. Plasma Processes and Polymers, 2022, 19, .	3.0	3
192	Selective Adsorption and Photocatalytic Cleanâ€Up of Oil by TiO ₂ Thin Film Decorated with pâ€V ₃ D ₃ Modified Flowerlike Ag Nanoplates. Advanced Materials Interfaces, 2022, 9, .	3.7	3
193	Chemical interaction at copper/polyaniline interfaces. Synthetic Metals, 2001, 121, 1317-1318.	3.9	2
194	Modification of a metal nanoparticle beam by a hollow electrode discharge. Journal of Vacuum Science and Technology A: Vacuum, Surfaces and Films, 2016, 34, 021301.	2.1	2
195	Controlling the flux of reactive species: a case study on thin film deposition in an aniline/argon plasma. Scientific Reports, 2020, 10, 15913.	3.3	2
196	Metal-polymer interfaces. , 0, , .		1
197	Hierarchical Structures: Photocatalytic Growth of Hierarchical Au Needle Clusters on Highly Active TiO ₂ Thin Film (Adv. Mater. Interfaces 15/2018). Advanced Materials Interfaces, 2018, 5, 1870074.	3.7	1
198	Comparative Analysis of the Nucleation and Growth of Copper on Different Low-k Polymers. Materials Research Society Symposia Proceedings, 2001, 714, 811.	0.1	0

#	Article	IF	CITATIONS
199	Spectroelectrochemical and morphological studies of the ageing of silver nanoparticles embedded in ultra-thin perfluorinated sputter deposited films. Thin Solid Films, 2014, 571, 161-167.	1.8	0
200	Frontispiece: Post-Synthetic Decoupling of On-Surface-Synthesized Covalent Nanostructures from Ag(111). Angewandte Chemie - International Edition, 2016, 55, .	13.8	0
201	Carbographite Buckypaper: A Flexible Oxygenated Carbographite Nanofilamentous Buckypaper as an Amphiphilic Membrane (Adv. Mater. Interfaces 8/2018). Advanced Materials Interfaces, 2018, 5, 1870036.	3.7	0

202 Superhydrophobic Surfaces: Superhydrophobic 3D Porous PTFE/TiO2 Hybrid Structures (Adv. Mater.) Tj ETQq0 0 0 rgBT /Overlock 10 Tf

203	Selective Adsorption and Photocatalytic Cleanâ€Up of Oil by TiO ₂ Thin Film Decorated with pâ€V ₃ D ₃ Modified Flowerlike Ag Nanoplates (Adv. Mater. Interfaces 14/2022). Advanced Materials Interfaces, 2022, 9, .	3.7	0	
-----	--	-----	---	--